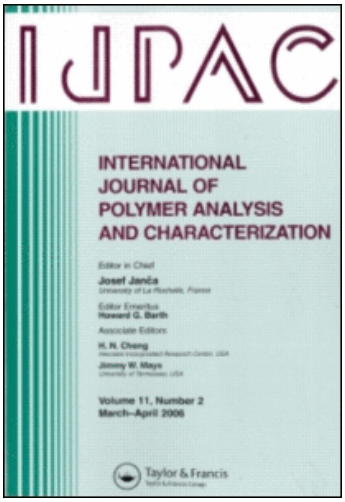

International Journal of Polymer Analysis and Characterization
Publication details, including instructions for authors and subscription information:
http://www.informaworld.com/smpp/title~content=t713646643

Organic-Inorganic Hybrid Materials X: Characterization and Degradation of Hydroxyl-Containing Fluorinated Polyimide-Silica Hybrids

T. C. Chang[a]; G. P. Wang[a]; H. C. Tsai[a]; Y. S. Hong[a]; Y. S. Chiu[b]
[a] Department of Applied Chemistry, Chung Cheng Institute of Technology. NDU, Tahsi, Taoyuan, Taiwan [b] Chemical Systems Research Division, Chung Shan Institute of Science and Technology, Taoyuan, Taiwan

Online publication date: 27 October 2010

To cite this Article Chang, T. C. , Wang, G. P. , Tsai, H. C. , Hong, Y. S. and Chiu, Y. S.(2003) 'Organic-Inorganic Hybrid Materials X: Characterization and Degradation of Hydroxyl-Containing Fluorinated Polyimide-Silica Hybrids', International Journal of Polymer Analysis and Characterization, 8: 3, 157 — 174
To link to this Article: DOI: 10.1080/10236660304877
URL: http://dx.doi.org/10.1080/10236660304877

International Journal of Polymer Anal. Charact., 8: 157–174, 2003

1023-666X/03 $12.00 + .00
DOI: 10.1080/10236660390128328

Taylor & Francis
Taylor & Francis Group

Organic-Inorganic Hybrid Materials X: Characterization and Degradation of Hydroxyl-Containing Fluorinated Polyimide-Silica Hybrids

T. C. Chang, G. P. Wang, H. C. Tsai, and Y. S. Hong
Department of Applied Chemistry,
Chung Cheng Institute of Technology, NDU,
Tahsi, Taoyuan, Taiwan

Y. S. Chiu
Chemical Systems Research Division,
Chung Shan Institute of Science and Technology,
Taoyuan, Taiwan

Hydroxyl-containing fluorinated polyimide-silica hybrid materials (FPI-SiO_2) were obtained using the sol-gel technique by polycondensation of tetramethoxysilane (TMOS) in 3-aminopropylmethyl diethoxysilane (APrMDEOS)-terminated amic acid solution. Infrared, ^{29}Si-, and ^{13}C-NMR spectroscopy and thermogravimetric analysis (TGA) were used to study hybrids containing various proportions of TMOS. The microstructure and chain mobility of the hybrids was investigated by spin-lattice relaxation time in rotating frame ($T_{1\rho}^{H}$) measurements. The apparent activation energy (E_a) for degradation of the hybrids was studied by Friedman and van Krevelen methods.

Received 24 March 2001; accepted 11 May 2001.

The authors thank the National Science Council of the Republic of China for financial support (NSC 90-CS-7-014-001). We would also like to thank Miss S. Y. Fang (Tsing Hua University) for help performing NMR measurements and Mr. Y. C. Lin (Chung Shan Institute of Science and Technology) for help performing TGA measurements.

Address correspondence to Te-Chuan Chang, Department of Applied Chemistry, Chung Cheng Institute of Technology, NDU, Tahsi, Taoyuan, Taiwan 335. E-mail: techuan@ccit.edu.tw

Keywords: Polyimide; Silica; Hybrids; Relaxation; Degradation

INTRODUCTION

Organic polymers combined with inorganic oxides using variations of the sol-gel method have become prevalent during the past decade as a means of preparing organic-inorganic hybrid materials[1]. The new hybrid materials could have a controllable combination of the properties of both organic polymers and inorganic glasses[2]. Polyimides (PIs) are of great interest for high-performance applications since they exhibit outstanding dielectric and mechanical properties at elevated temperatures[3]. However, PIs exhibit relatively high values of water sorption ($\sim$4 wt%) and coefficients of thermal expansion ($\sim 5 \times 10^{-5}\,K^{-1}$), impeding electronic applications[4]. Silica (SiO_2), exhibiting very low values of water sorption ($\sim$0 wt%) and coefficients of thermal expansion ($\sim 5 \times 10^{-7}\,K^{-1}$), would be more suited for electronic applications, but dielectrical properties, planarizability, and patternability of silica are inferior to those of PIs.

Hybrid polyimide-silica materials (PI-SiO_2) offering favorable properties of both polyimides and silica are therefore in great demand. Research on a PI-SiO_2 hybrid was first reported in the early 1990s. Nandi et al.[5] produced PI-SiO_2 hybrids by mixing solutions of pyromellitic anhydride, diaminodiphenyl ether, and silicon tetraalkoxides. They relied only on physical interactions between the inorganic and organic phases, which accordingly become opaque at low-weight percentage silica owing to phase separation on the micron scale. Morikawa et al.[6–8] subsequently prepared the PI-SiO_2 hybrids by means of polyamic acid–containing pendant alkoxylsilane groups along the chains that create bonding sites between the polymer backbone and the silica. The authors found that the movement of the PI chains in the matrix is restricted. Wang et al.[9,10], Mascia et al.[11–15], and Smaihi et al.[16,17] further reported the use of organically substituted alkoxysilane to bond between the polyimide and the silica. The addition of a small amount of the bonding agents was found to improve the strengths of these hybrid materials. Sysel et al.[18] conducted experiments that showed that silane-terminated poly(amic acids) with molecular weight less than 10,000 g/mol were suitable for preparing transparent hybrid materials with silica content higher than 10 wt%.

Hobson and Shea[19] synthesized a new hybrid materials that were prepared by condensation of bisimide monomers containing pendant triethoxysilyl groups. The advantage of this process is the homogeneous distribution of the silica in organic matrix. We also produced hybrid materials via a sol-gel technique by mixing tetramethoxysilane (TMOS)

with a 3-aminopropylmethyl diethoxysilane (APrMDEOS)-terminated amic acid[20]. Four components with different molecular mobility in PI-SiO_2 hybrids were observed by spin-spin relaxation measurements. Moreover, the degraded products of the siloxane segments had a retarding effect on degradation of imide segments. However, we characterized the dynamics and stability of the hydroxyl-containing fluorinated poly(siloxane imide)[21]. These copolymers may become good candidates for sorbent polymers for basic vapors on surface acoustic wave (SAW) sensors[22,23]. However, it is difficult to attach a sorbent polymer coating on an SAW surface. For example, the surface of the SAW device was modified by plasma activation and using a coupling agent to form stable thin films[24]. Therefore, a series of new hybrid materials, prepared by mixing a solution of TMOS and hydroxyl-containing fluorinated amic acid terminated with diethoxysilane via sol-gel method, may be a good choice. The effect of the silica content on the dynamics and stability of the resulting hybrids are characterized in the present study.

EXPERIMENTAL

Materials

4,4′-(Hexafluoroisopropylidene) diphthalic anhydride (6FDA) and 2,2′-bis(3-amino-4-hydroxyl phenyl) hexafluoropropane (AHHFP) were obtained in high purity from Chriskev Inc. and dried under a vaccum for 24 h at 120° and 70°C, respectively. Tetramethoxysilane (TMOS) and 3-aminopropylmethyl diethoxysilane (APrMDEOS) were obtained from the Tokyo Chemical Industry Co. and used without further purification. *N,N*-Dimethylacetamide (DMAc, Aldrich) and toluene were distilled under a vacuum. Deionized water (18 MΩ) was used for their hydrolysis.

Preparation of FPSI-SiO_2 Hybrids

The general synthetic scheme of the FPI-SiO_2 hybrid materials is depicted in Scheme 1. The preparation of 3-aminopropylmethyl diethoxysilane–terminated amic acid with a solid concentration of 15 wt% was conducted at room temperature under nitrogen. A solution of 6FDA in a 3:1 (v/v) DMAc/toluene mixture was added to a solution of AHHFP in a cosolvent mixture (DMAc:toluene = 3:1) in a round-bottomed flask with a stirring magnet. After 30 min the APrMDEOS was added and the clear solution was stirred for 24 h. The resulting viscous orange pale amic acid solution was then obtained.

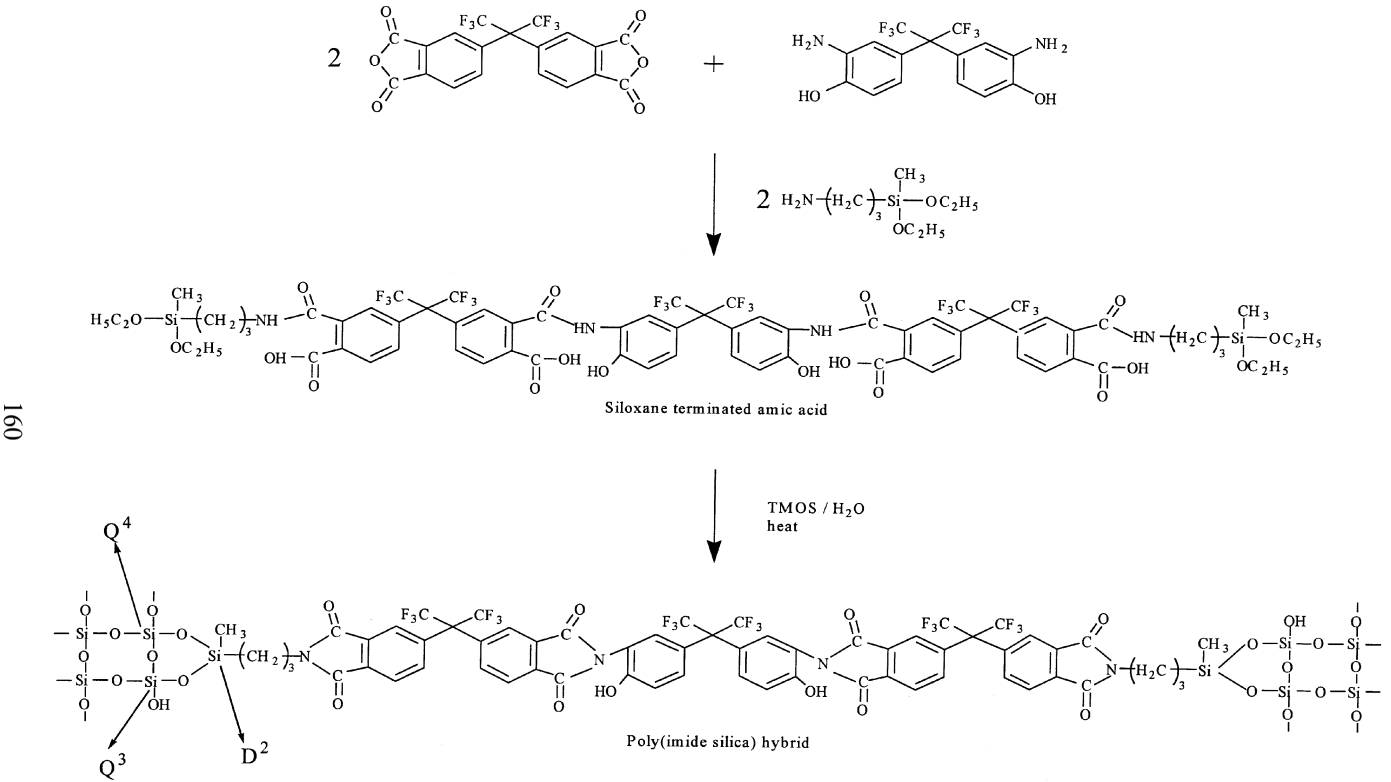

SCHEME 1. General synthetic scheme of FPI-SiO_2 hybrid materials.

The desired amount of water and TMOS were added to the amic acid solution and stirred for an additional 24 h at room temperature. The resulting homogeneous solution was poured onto a Teflon dish. After drying at 60°C for 24 h under atmospheric pressure, the film was then heated 3 h at 100°C, 3 h at 200°C, 2 h at 290°C, and 2 h at 190°C under a vacuum. Hybrid materials were designated so that, for example, 6C-25, 6C-30, 6C-35, 6C-40, and 6C-45 denote amic acid reacted with about 25, 30, 35, 40, and 45 wt% of TMOS, respectively, in which the molar ratio of $[H_2O]/[TMOS]$ was 6. The FPSI hybrid 6C without addition of TMOS was synthesized via a similar procedure for comparison.

Characterization of FPSI-SIO_2 Hybrids

The infrared (IR) spectra of samples dispersed in dry KBr pellets were recorded between 4000 and 550 cm^{-1} on a Bomen DA 3.002 FTIR spectrometer. Imidization was confirmed by the IR spectra of samples. The ^{29}Si-NMR and ^{13}C-NMR spectra of the solid hybrids were determined (Bruker MSL-400) by using the cross-polarization combined with magic angle spinning (CP/MAS) technique. The ^{29}Si-NMR spectrum provides a unique way to follow the hydrolysis and condensation reactions of silicon alkoxides. The nomenclature of D^i and Q^i is taken from Glaser and Wilkes[25] where i refers to the number of -O-Si groups bounded to the silicon atom of interest. D^i and Q^i denote species that have two and no organic side group, respectively. CP contact time studies can produce the Si-H polarization transfer constant (T_{SiH}). The ^{1}H-^{29}Si spin contact time with the Hartmann-Hahn condition fulfilled in the rotating frame was typically about 5 ms, but was optimized in the range between 0.5 and 20 ms. The characteristics and kinetics of degradation of the hybrids were measured by a Perkin-Elmer TGA-7 at heating rate of 10°C/min under air and nitrogen. The sample weight was about 10 mg, and the gas flow rate was kept at 100 mL/min.

RESULTS AND DISCUSSION

Materials Characterization

The hybrids present the silanol group formed during the hydrolysis of alkoxy groups (Si-OCH_3) in APrMDEOS and TMOS, and that induces cross-linked three-dimensional (3-D, Q^i) network materials. However, the hybrid 6C presents two siloxane bonds and one methyl group bonded to a silicon atom, giving a two-dimensional network material. The theoretical

schematic structures of the hybrids are shown in Scheme 1. IR and solid-state ^{29}Si- and ^{13}C-NMR provided evidence for the formation of hybrid network materials.

The IR spectra of hybrid materials containing various proportions of silica are shown in Figure 1. All hybrids present the characteristic imide peaks at 1778 (imide C=O symmetric stretching), 1712 (imide C=O asymmetric stretching), 1392 (C-N stretching), and 722 cm^{-1} (imide ring deformation). The Si-O-Si vibration (1059 cm^{-1}) is small in 6C hybrid, Figure 1(A), but this absorption band is broader with increasing silica content for other hybrids, Figure 1(B–F). This implies the condensation of the already hydrolyzed TMOS to form the 3-D Si-O-Si network[26]. The absorptions in the range 3700–3200 cm^{-1} and 966 cm^{-1} are the characteristic band of silanol groups (Si-OH) that are formed during the hydrolysis of alkoxy groups in APrMDEOS or TMOS. The carbonyl

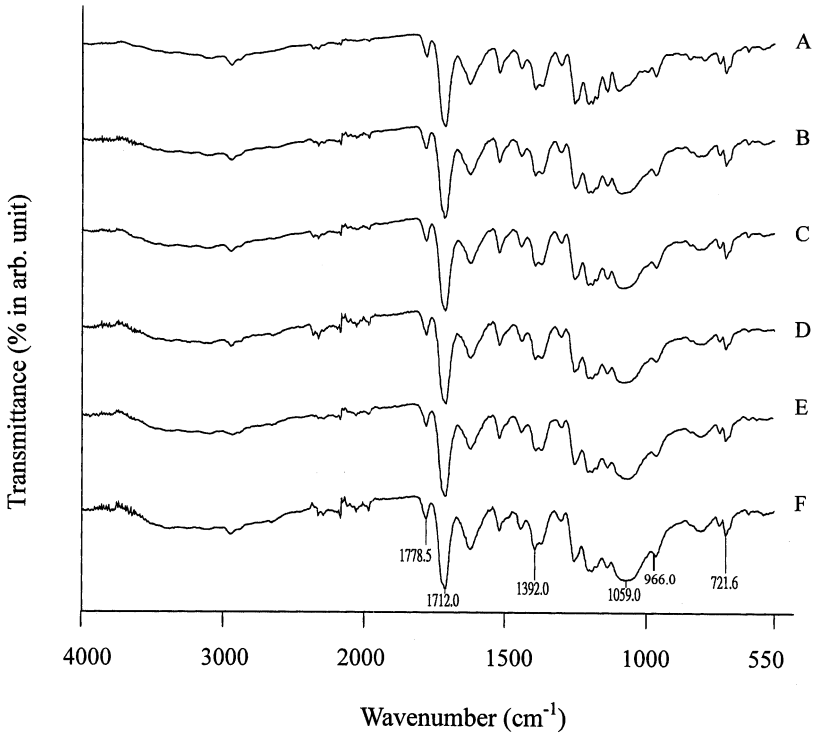

FIGURE 1 Infrared spectra of the FPI-SiO_2 hybrid materials. (A) 6C, (B) 6C-25, (C) 6C-30, (D) 6C-35, (E) 6C-40, and (F) 6C-45.

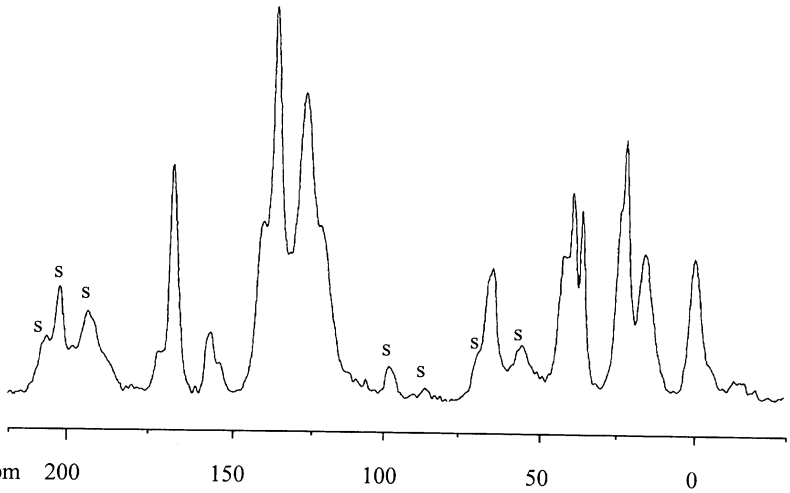

FIGURE 2 CP-MAS ^{13}C-NMR spectrum of the 6C hybrid (s: side band).

stretching bands in FPI-SiO_2 hybrids are shifted to lower wave number (1778 and 1712 cm^{-1}) as observed from a comparison with a five-member imide ring (1782 and 1724 cm^{-1}). This result indicates that a hydrogen bond is formed between the hydroxyl, silanol, and carbonyl groups in FPI-SiO_2 hybrids[27].

The ^{13}C-CP/MAS NMR spectra of FPI-SiO_2 hybrids are nearly identical and have sufficient resolution to identify peaks. Figure 2 shows the ^{13}C CP/MAS NMR spectrum of 6C hybrid. A set of peaks are observed at 166, 154, 140–118, and 65 ppm that arise from the imide carbonyl, aryl carbons with hydroxyl groups, various aromatic carbons, and quartet carbons, respectively[17]. Moreover, the other set of peaks are observed at around 41, 21, 15, and –1.0 ppm that correspond to -NCH_2-, -CH_2-, -CH_2Si-, and -$SiCH_3$, respectively.

The ^{29}Si-NMR spectra of FPI-SiO_2 hybrids at the mixing time τ of 5 ms (Figure 3) show two peaks about at -20.8 and -108 ppm corresponding to D^2 and Q^4, respectively. Moreover, a shoulder at about -100 ppm corresponds to a Q^3 structure[20]. The D^2 structures and Q^i structures ($i = 2$ and 3) can be attributed to the silicon in the siloxane sequence and 3-D silica network, as shown in Scheme 1. The result of abundant Q^4 structures implies that the hydroxyl-containing fluorinated amic acid enhances the degree of condensation (D_C) of the TMOS. Table I lists the D_C values (~95%) that are determined by a quantitative analysis of the D^2, Q^3, and Q^4 resonance signals. Interestingly, D_C decreases with increasing silica content.

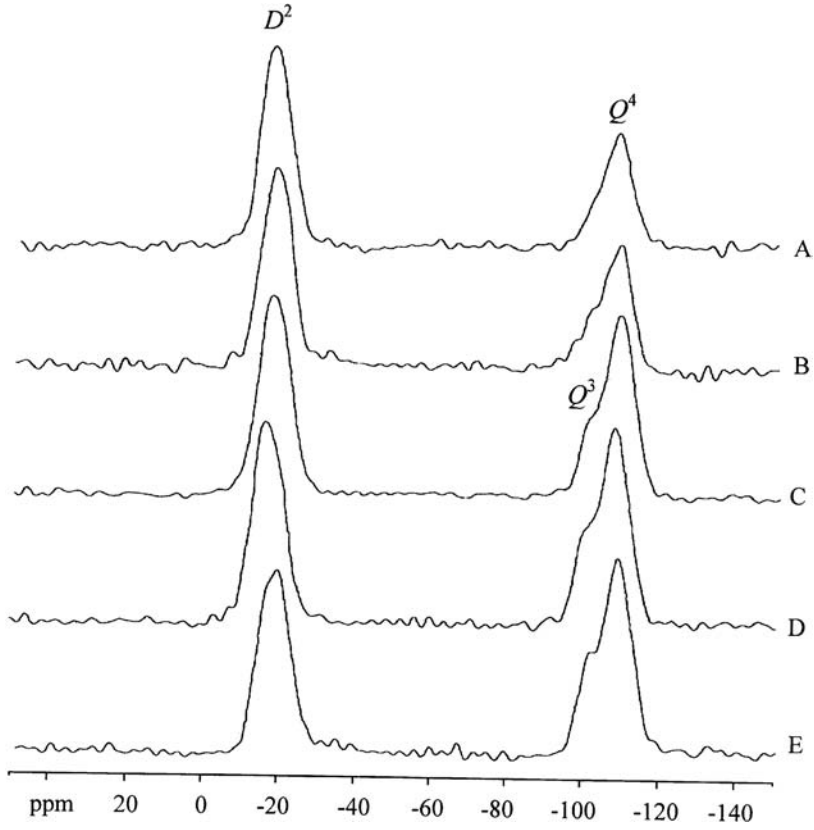

FIGURE 3 CP-MAS ^{29}Si NMR spectra of various hybrid materials at mixing time τ of 5 ms. (A) 6C-25, (B) 6C-30, (C) 6C-35, (D) 6C-40, and (E) 6C-45.

Cross-Polarization Process

In the conventional CP process under Hartmann-Hahn conditions, ^{1}H and ^{29}Si spin systems are spin-locked in the rotating frames and thermally in contact with each other, thus exchanging their energies. The respective spin systems also exchange energies with the surrounding thermal reservoir, the so-called lattice. Figure 4 gives an example of the effect of contact time (t) on the ^{29}Si resonance of 6C-35 hybrid. Intensities in the Figure 4 reflect local cross-polarization dynamics that may vary from site to site. According to the simple theory in this CP process, magnetization, $M_c(t)$, is expressed as a function of the contact time as follows[28]:

$$M_c(t) = M_e[\exp(-t/T_{1\rho}^H) - \exp(-t/T_{\mathrm{SiH}})] \quad (1)$$

Here, M_e is the ^{29}Si equilibrium magnetization obtained when both spin systems fully interact with each other without any energy exchange with the lattice. T_{SiH} is the time constant for the energy exchange between ^{1}H and ^{29}Si spin systems and $T_{1\rho}^H$ is the spin-lattice relaxation time in

TABLE I T_{SiH} and $T_{1\rho}^H$ values of the respective resonance lines of FPI-SiO_2 hybrid, and L values of hybrids materials

		T_{SiH} (ms)			$T_{1\rho}^{\mathrm{H}}$ (ms)			
Hybrids	D_C (%)[a]	D^2	Q^3	Q^4	D^2	Q^3	Q^4	$T_{1\rho,\ \mathrm{av(ms)/L(nm)}}^{\mathrm{H}}$
6C-25	95.34	2.82	2.48	1.76	18.50	42.41	49.16	36.69/4.69
6C-30	95.41	2.80	2.18	1.69	19.44	22.29	42.00	27.91/4.09
6C-35	95.18	2.56	2.25	1.60	13.85	24.04	24.58	20.83/3.53
6C-40	94.60	2.61	2.38	1.63	13.36	24.74	32.10	23.40/3.75
6C-45	94.21	2.74	2.49	1.65	13.73	18.82	31.56	21.37/3.58

[a]The degree of condensation of the APrMDEOS and TMOS.

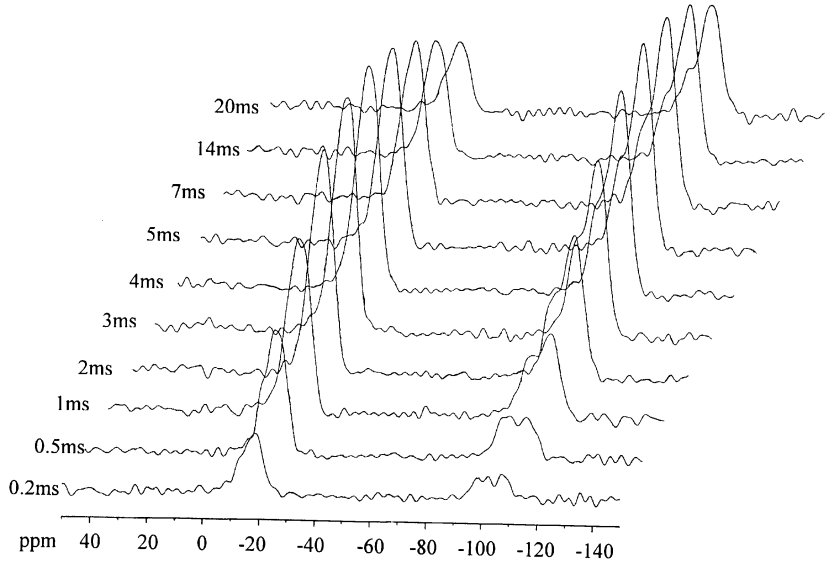

FIGURE 4 Stacked plot of the CP-MAS ^{29}Si NMR spectra of 6C-35 hybrid as a function of contact time.

rotating frame. This equation indicates that the ^{29}Si magnetization appears at the rate of the order of $(T_{SiH})^{-1}$ and disappears at the rate of $(T^{H}_{1\rho})^{-1}$. The rate of polarization transfer is dependent upon the distance between silicon and hydrogen atoms and on local motion. Silicon atoms, which, far from protons are very mobile, will take a longer time to cross-polarize.

Figure 5 shows a semilogarithmic plot of the peak intensity as a function of the contact time for the silicon in the 6C-35 hybrid. A steeper slope is an indication of faster transfer of magnetization (shorter T_{SiH}) or faster relaxation by spin diffusion (shorter $T^{H}_{1\rho}$). The T_{SiH} and $T^{H}_{1\rho}$values estimated by curve-fitting are summarized in Table I. The D^2 structures with the largest number of relatively close protons should

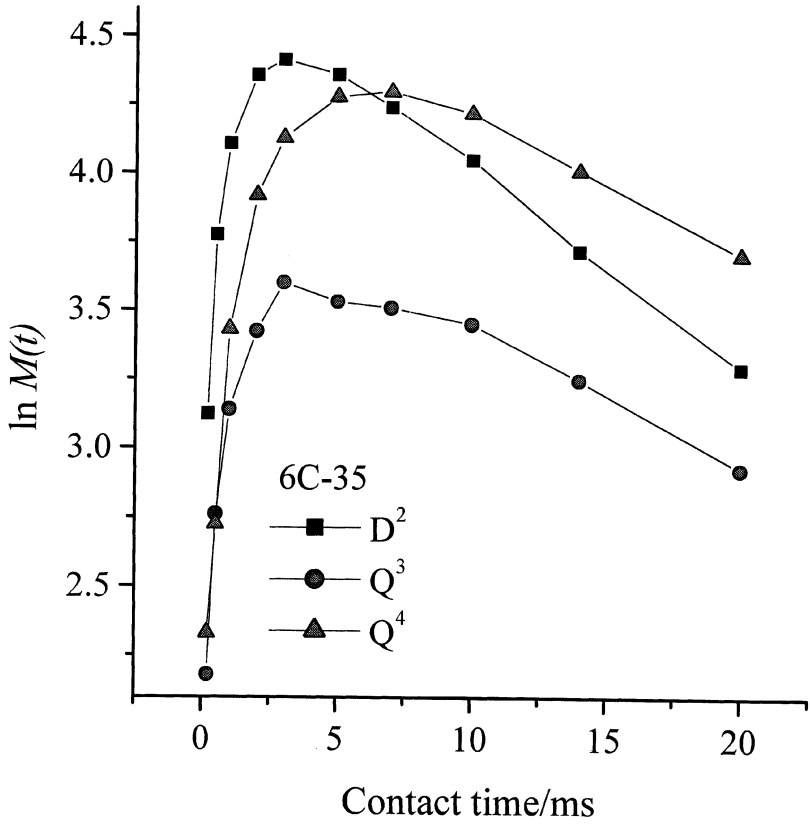

FIGURE 5 Semilogarithmic plot of the peak intensity of the D^2, Q^3, and Q^4 species shown in Figure 4 as a function of contact time.

exhibit the shortest T_{SiH} values, while Q^4 structures lacking directly bonded protons should have the longest T_{SiH} as compared to the D^2 and Q^3 structures. However, the T_{SiH} values of the FPSI-SiO_2 hybrids (Table I) are in the order D^2 ($\sim$2.7 ms) > Q^3 ($\sim$2.4 ms) > Q^4 ($\sim$1.7 ms). Thus, the converse results suggest that the rate of polarization transfer in FPSI-SiO_2 hybrids is dependent in a major way upon the local motion. The greater motion of the D^2 structures could result in weak dipolar coupling and longer T_{SiH} relaxations. Moreover, the linear curve of Q^4 species in Figure 5 suggests that large-scale phase separation does not occur in these materials. The spin-diffusion path length (L) can be estimated using the following equation:[28]

$$L = (6D\,T_{1\rho}^{H})^{1/2} \tag{2}$$

Here D is the effect spin-diffusion coefficient depending on the average proton-to-proton distance as well as dipolar interaction; it has a typical value of the order of 10^{-16} m^2s^{-1}. The $T_{1\rho}^{H}$ average values (Table I) of the hybrids decrease roughly with increasing the silica content, and the L values ($\sim$5.5 nm) in hybrids then decrease (Table I). The reduction in spin-diffusion path length may be associated with a reduced free volume as silica content increases[29].

Thermal Analysis

The TGA curves of hybrid materials under nitrogen are shown in Figure 6, which are reflected in two main peaks in differential weight loss curves (DTG). The first weight loss steps are observed below 400°C, corresponding to the release of ethanol and water during heating, which are evidence of incompletion of the sol-gel process[12]. The degradation step above 400°C corresponds to the decomposition of organic siloxane and imide part. The final char yield (Y_c) at 800°C increases with increasing silica content. The characteristic parameters of thermal degradation (10°C/min) for the FPI-SiO_2 hybrids are listed in Table II. Figure 7 shows the TGA curves of FPI-SiO_2 hybrids under air, which also reflect two main degraded steps. The char yields (Y_c) of the hybrids in thermooxidative degradation are markedly less than those of the calculated values (Table III). The result may be due to other vaporized silicon products produced in air atmosphere[30].

The degree of conversion α is defined as the ratio of actual weight loss to total weight loss. Therefore, the rate of degradation $d\alpha/dt$, dependent on temperature and weight of the sample, is given by Equation (3):

$$d\alpha/dt = k(T) \times f(\alpha) \tag{3}$$

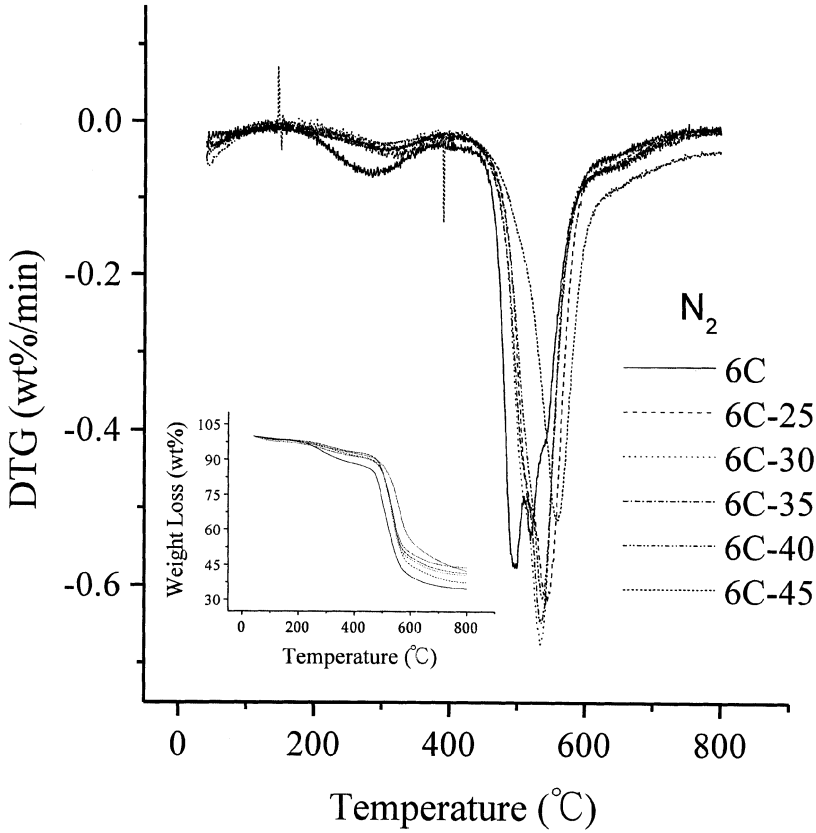

FIGURE 6 TGA and DTG thermograms of the FPI-SiO_2 hybrid materials undergoing thermal degradation (10°C/min).

where $k(T)$ is the rate constant and $f(\alpha)$ is the conversion functional relationship. If $k(T) = A\exp(-E_a/RT)$ and $f(\alpha) = (1-\alpha)^n$, then Equation (3) can be expressed as:

$$d\alpha/dt = [A\exp(-E_a/RT)](1-\alpha)^n \quad (4)$$

where A, E_a, R, T, and n represent preexponential factor, activation energy, gas constant, temperature, and reaction order, respectively. The apparent activation energy E_a values of degradation can be estimated from the Friedman method according to the following equation[31]:

$$\ln(d\alpha/dt) = \ln A + n\ln(1-\alpha) - E_a/RT \quad (5)$$

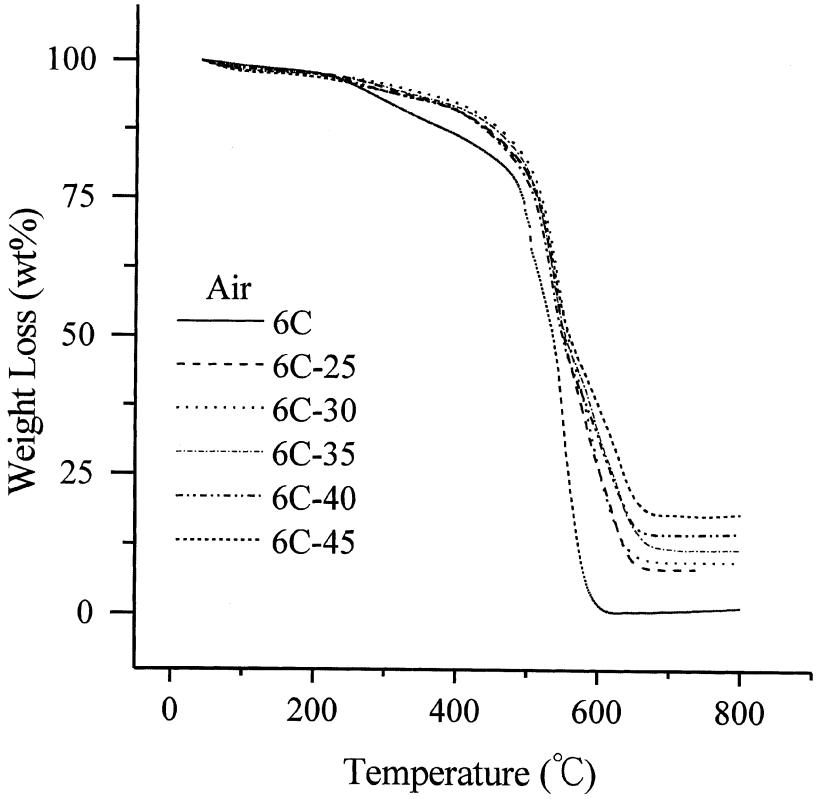

FIGURE 7 TGA and DTG thermograms of the FPI-SiO_2 hybrid materials undergoing thermooxidative degradation (10°C/min).

Table II and Table III list the E_a values of the siloxane segments in thermal and thermooxidative degradation, respectively. We found that the E_a value in thermal degradation decreases with increasing silica content, while that in thermooxidative degradation increases.

By integrating Equation (4) and introducing the initial condition of $\alpha = 0$ at $T = T_0$ the following expression is obtained:

$$g(\alpha) = \int_0^{\alpha} \frac{d\alpha}{(1-\alpha)^n} = \frac{A}{q} \int_{T_0}^{T} \exp\left(\frac{-E_a}{RT}\right) dT \qquad (6)$$

where q is heating rate (dT/dt). The reaction order n for degradation in this work is determined by the Kissingers' equation[20]. The value of n in the initial second step, corresponding to the scission of siloxane chain, is

TABLE II Characteristic parameters of thermal degradation (10°C/min) for hybrid materials

	Stage 1		Stage 2			
Hybrids	T (°C)	W (wt%)[a]	T (°C)	W (wt%)	Y_c (wt%)[b]	E_a (kJ/mol)[c]
6C	40–399	11.83	399–804	53.48	34.69	121 (267)[a]
6C-25	40–412	8.61	412–804	53.97	37.42	115 (212)
6C-30	40–414	7.01	414–800	52.46	40.43	122 (245)
6C-35	40–383	6.75	383–765	52.01	41.23	130 (181)
6C-40	40–393	8.87	393–714	47.29	43.84	111 (195)
6C-45	40–416	7.83	416–789	49.95	42.22	74 (119)

[a]Weight loss. [b]Char yield. [c]Apparent activation energy evaluated by the van Krevelen method. [d]The E_a values in parentheses are evaluated by the Friedman method.

TABLE III Characteristic parameters of thermooxidative degradation (10°C/min) for hybrid materials

	Stage 1		Stage 2			
Hybrids	T (°C)	W (wt%)[a]	T (°C)	W (wt%)	Y_c (wt%)[b]	E_a (kJ/mol)[c]
6C	40–433	16.07	433–646	83.38	0.54 (7.34)	97 (101)
6C-25	40–330	6.26	330–707	85.50	8.24 13.75)	118 (148)
6C-30	40–358	6.20	358–704	84.19	9.54 (14.74)	119 (149)
6C-35	40–361	7.08	361–724	81.07	11.71 (15.66)	136 (136)
6C-40	40–351	7.27	351–714	78.28	14.46 (16.50)	123 (153)
6C-45	40–350	7.09	350–720	74.92	18.00 (17.30)	122 (180)

[a]Weight loss. [b]Char yield. [c]Apparent activation energy evaluated by the van Krevelen method. [d]The Y_c values in parentheses are evaluated by calculation. [e]The E_a values in parentheses are evaluated by the Friedman method.

independent of the TMOS content and is about 1.26. For n not equal to zero or unit,

$$g(\alpha) = \int_0^{\alpha} \frac{d\alpha}{(1-\alpha)^n} = -\ln(1-\alpha) = -\frac{1-(1-\alpha)^{1-n}}{1-n} \qquad (7)$$

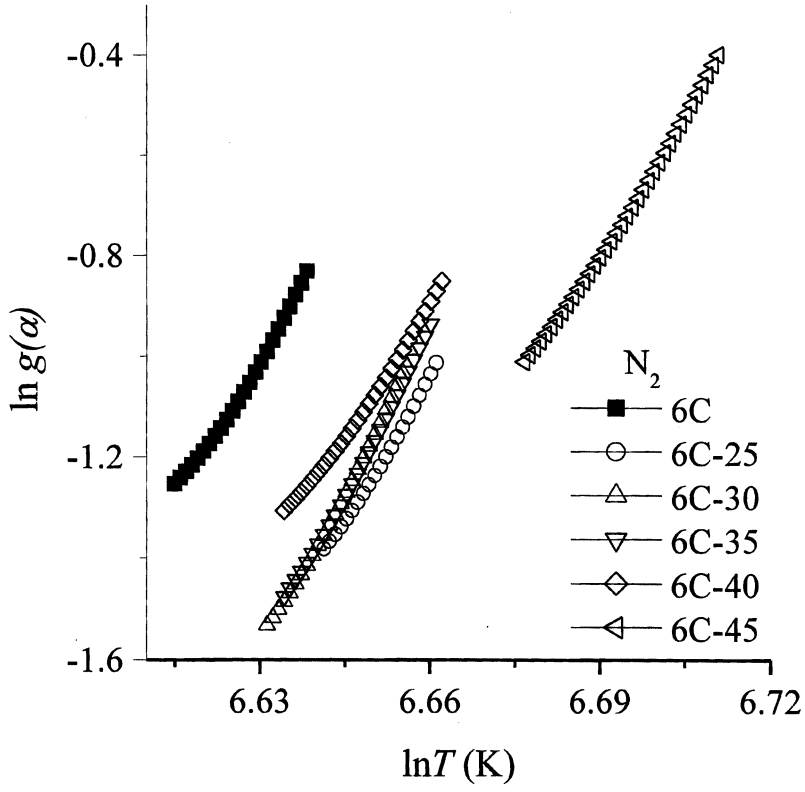

FIGURE 8 Plot of $\ln g(\alpha)$ versus $\ln T$ for thermal degradation (10°C/min) of siloxane segments in the FPSI-SiO_2 hybrid materials.

The integrating method used by van Krevelen[20] is expressed by:

$$n \neq 1 \qquad \ln g(\alpha) = \ln\left[\frac{A(0.368/T_m)^x}{q(\chi+1)}\right] + (\chi+1)\ln T \qquad (8)$$

Here $\chi = E_a/RT_m$, and T_m is the temperature at the maximum rate of weight loss. Therefore, E_a can be obtained from the slopes in a plot of $\ln g(\alpha)$ versus $\ln T$, as shown in Figures 8 and 9. The reduction of the E_a values in thermal degradation (Table II) reveals that silica may favor the aliphatic *n*-propyl segment degradation[32]. This may be associated with the higher thermal conductivity of the silica (5 mcal/cm s °C) than that of polyimide (0.4 mcal/cm s °C)[33]. However, the enhancement of the E_a values in thermooxidative degradation (Table III) implies that the addition of the silica fraction is effective in decreasing the free volume of the fluorinated polyimide.

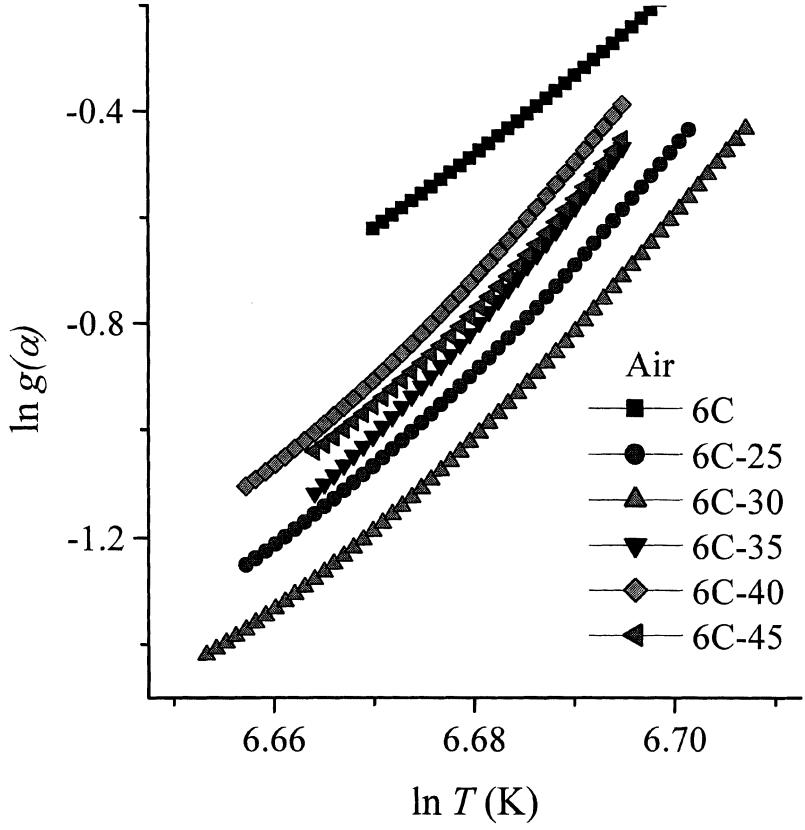

FIGURE 9 Plot of ln g(α) versus ln T for thermooxidative degradation (10°C/min) of siloxane segments in the FPI-SiO_2 hybrid materials.

The oxygen permeability and diffusion coefficients of the FPI-SiO_2 hybrids are then decreased[29].

CONCLUSIONS

Hydroxyl-containing fluorinated poly(siloxane imide)-silica hybrid materials (FPI-SiO_2) have been prepared using the sol-gel technique by condensation of tetramethoxysilane in 3-aminopropylmethyl diethoxy-silane–terminated amic acid solution. Infrared, ^{29}Si-, and ^{13}C-NMR spectroscopy and thermogravimetric analysis (TGA) were used to study

hybrids containing various proportions of TMOS. The abundant Q^4 structures implied that the degree of condensation of TMOS was enhanced by hydroxyl-containing fluorinated amic acid. The T_{SiH} values of the FPI-SiO_2 hybrids were in the order $D^2 > Q^3 > Q^4$, suggesting that the rate of polarization transfer in FPI-SiO_2 hybrids was dependent on the local motion.

The apparent activation energies E_a of degradation in hybrids were evaluated by the van Krevelen method. The E_a values of the FPI-SiO_2 hybrids in thermal degradation decreased with increasing silica content, whereas those in thermooxidative degradation decreased. The results suggested that silica enhanced the aliphatic *n*-propyl segment degradation and the silica fraction is effective in decreasing the free volume of the hybrid materials.

REFERENCES

[1] Mark, J. E., Lee, C. Y. C., and Bianconic, P. A. (1995). In: *Hybrid Organic-Inorganic Composites*, ACS Symposium Series 585, American Chemical Society, Washington, DC.
[2] Wen, J. G. and Wilkes, L. (1996). *Chem. Mater.,* **8**, 1667.
[3] Sroog, C. A. (1991). *Progr. Polym. Sci.,* **16**, 561.
[4] Numata, S. and Kinjo, N. (1998). *Polym. Eng. Sci.,* **28**, 906.
[5] Nandi, M., Conklin, J. A., Salvati, L., and Sen, A. (1991). *Chem. Mater.,* **3**, 210.
[6] Morikawa, A., Iyoku, Y., Kakimoto, M., and Imai, Y. (1992). *Polym. J.,* **24**, 107.
[7] Morikawa, A., Iyoku, Y., Kakimoto, M., and Imai, Y. (1992). *J. Mater. Chem.,* **2**, 679.
[8] Morikawa, A., Yamaguchi, H., Kakimoto, M., and Imai, Y. (1994). *Chem. Mater.,* **6**, 913.
[9] Wang, S., Ahmad, Z., and Mark, J. E. (1994). *Macromolecular Rep.,* **A31**, 411.
[10] Wang, S., Ahmad, Z., and Mark, J. E. (1994). *Chem. Mater.,* **6**, 943.
[11] Mascia, L. and Kioul, A. (1994). *J. Mater. Sci. Lett.,* **13**, 641.
[12] Kioul, A. and Mascia, L. (1994). *J. Non-Cryst. Solids*, **175**, 169.
[13] Mascia, L. and Kioul, A. (1995). *Polymer*, **36**, 3649.
[14] Mascia, L. and Zhang, Z. (1996). *Composites Part A*, **27A**, 1211.
[15] Xenopoulos, C., Mascia, L., and Zhang, Z. (1998). *Mater. Sci. Eng.,* **C6**, 99.
[16] Schrotter, J. C., Smaihi, M., and Guizard, C. (1996). *J. Appl. Polym. Sci.,* **61**, 2137.
[17] Smaihi, M., Schrotter, J. C., Lesimple, C., Prevost, I., and Guizard, C. (1999). *J. Membr. Sci.,* **161**, 157.
[18] Sysel, P., Pulec, R., and Maryska, M. (1997). *Polym. J.,* **24**, 107.
[19] Hobson, S. and Shea, T. K. J. (1997). *Chem. Mater.,* **9**, 616.
[20] Wu, K. H., Chang, T. C., Wang, Y. T., and Chiu, Y. S. (1999). *J. Polym. Sci. Part A: Polym. Chem.,* **37**, 2275.
[21] Wang, G. P., Chang, T. C., Hong, Y. S., and Chiu, Y. S. (2001). *Int. J. Polym. Anal. Charact*. (in press).
[22] Grate, J. W., Kaganove, S. N., Patrash, S. J., Craig, R., and Bliss, M. (1997). *Chem. Mater.,* **9**, 1201.
[23] Grate, J. W., Patrash, S. J., Kaganove, S. N., and Wise, B. M. (1999). *Anal. Chem.,* **71**, 1033.

[24] McGill, R. A., Abraham, M. H., and Grate, J. W. (1994). *Chemtech*, **24**(9), 27.
[25] Glaser, R. H. and Wilkes, G. L. (1988). *Polym. Bull.,* **19**, 51.
[26] Avadhani, C. V., Chujo, Y., Kuraoka, K., and Yazawa, T. (1997). *Polym. Bull.,* **38**, 501.
[27] Ahn, T., Kim, M., and Choe, S. (1997). *Macromolecules*, **30**, 3369.
[28] Mehring, M. (1983). *Principles of High Resolution NMR in Solids*, 2nd ed., Springer, Berlin.
[29] Mikawa, M., Nagaoka, S., and Kawakami, H. (1999). *J. Memb. Sci.,* **163**, 167.
[30] Lopez, M. A., Martinez, L., Villareal, A., and Castillo, J. R. (1998). *Talanta*, **45**, 1211.
[31] Li, X. G., Huang, M. R., and Bai, H. (1999). *J. Appl. Polym. Sci.,* **73**, 2927.
[32] Yilgor, I. and McGrath, J. E. (1988). *Adv. Polym. Sci.,* **86**, 1.
[33] Soane, D. S. and Martynenko, Z., ed. (1989). *Polymers in Microelectronics Fundamental and Applications*, Elsevier, Amsterdam, 159.